Validation of the Optimal Scale Selection Approach in Higher Dimensional Edge Extraction

Ji-Young Lim

Academic advisor:
Prof. Dr.-Ing. H. Siegfried Stiehl

Universität Hamburg
Fachbereich Informatik
Arbeitsbereich Kognitive Systeme

August, 2002

Abstract

In this report, we present the results of a validation study in which we investigated how well the experimental results obtained from the application of the developed framework for optimal scale-selection in higher dimensional edge extraction to test images match the theoretical results. We carry out the validation in two steps, i.e. with respect to the straight edge case and the circular edge case, and use several types of synthetic edge images in the experiments. In the straight edge case as well as in the circular edge case, the obtained experimental results are close to the theoretical results on the whole, though the experimental results slightly deviate from the theoretical ones, which may be rightfully assumed to be caused by an inevitable gap between a well-founded continuous theory and the implemented discrete case.

Zusammenfassung

In diesem Bericht präsentieren wir die Ergebnisse einer experimentellen Validierungsstudie zur Anwendbarkeit des von uns entwickelten Ansatzes zur optimalen Skalenbestimmung bei der Extraktion von Kantenstrukturen aus mehrdimensionalen Grauwertbildern. In der Studie werden verschiedene synthetische Bilder untersucht, die auf zwei unterschiedlichen Kantenmodellen basieren: einem Modell für eine nichtgekrümmte Kante sowie einem Modell fur eine gekrümmte Kante. Die Studie zeigt, daß die experimentellen Ergebnisse im allgemeinen gut mit den theoretisch erzielten Ergebnissen übereinstimmen. Die beobachteten Abweichungen sind hauptsächlich auf die Diskretisierung des entwickelten kontinuierlichen Ansatzes zur optimalen Skalenbestimmung zuruckzuführen.

Contents

1 Introduction

We have developed in [5] a theoretical framework for optimal scale selection in higher dimensional edge extraction. In this work, we validate the developed theoretical framework through investigating how well the experimental results obtained from application of the developed framework to an image match the theoretical result.

Since the optimal scale value (i.e. edge width) must be known a priori for our validation study, we use several types of synthetic edge images and control edge width in the experiments. For a given synthetic image, we apply the developed theoretical framework to this image, and inspect whether (or, respectively, how exactly) the result comes close to the expected theoretical result.

This report is organized as follows: In Section 2, we carry out the validation and present the obtained experimental results along with an assessment. Then, we summarize the major findings in Section 3.

2 Validation and Its Results

The theoretical result derived in [5, Sec. 5.2] is that an optimal scale value in higher dimensional edge extraction based on the fine-to-coarse multiscale tracking can be directly selected. The aim of this section is to validate the developed theoretical framework using synthetic images. Through this validation study, i) we intend to check for correctness of our theoretical derivation as well as our implementation, ii) we demonstrate in practice the principal behavior, and (iii) we can probe the limits for some extreme cases.

It is clear that a comprehensively full validation is beyond the scope of this thesis. This validation study is rather a first attempt for validating optimal scale selection approach in higher dimensional edge extraction.

2.1 Experimental Setting

We employ the non-maxima suppression approach by Canny [1] for higher dimensional edge extraction, for which we use the DSS kernel and its first-order odd-number-sized differencing kernel (i.e. $T_{\triangle_{odd}}$) both of which are validated in [6]. The developed framework is based on a classification of higher dimensional edges according to curvature (see for detail [5]), and thus its validation has to be carried out in two steps (i.e. with respect to the case of straight edge and the case of circular edge).

For a given synthetic image, we control the degree of edge width denoted as N by convolving the image with the DSS kernel, the variance (t_E) of which varies from $\frac{1}{3}$ to $\frac{13}{3}$ (i.e. $t_E = \frac{N}{3}, N = 1, 2, \cdots, 13$) in our experiment. Given a blurred synthetic image, we add three different levels of additive Gaussian noise, namely no noise ($\sigma = 0$), weak noise ($\sigma = 5.0$), and strong noise ($\sigma = 10.0$). While applying the developed framework for optimal scale selection to the blurred noisy synthetic image, we observe the response of the edge extraction scheme at edge loci as a function of t for checking whether the expected scale is selected indeed.

- The straight edge case

(a) S1 (b) S2 (c) S3 (d) S4

Figure 2.1: Synthetic images representing four different types of straight edge. The in-between-distance of parallel straight edge lines of S3 corresponds to 40 pixels, whereas the one of S4 corresponds to 20 pixels. The white line marks the edge locus to be observed. Recall that the degree of edge width denoted as N (or equivalently $t_E = \frac{N}{3}$: t_E corresponds to the variance of the DSS kernel) takes $2N + 1$ pixels (see for details [6, Sec. 2]).

We use four synthetic images representing four different types of a straight edge (see Fig. 2.1). S1 has a straight edge line with vertical orientation, whereas S2 contains a straight edge line with diagonal orientation. The experiments using S1 and S2 can reveal the principal behavior of the optimal scale selection with respect to two major orientations of a straight edge. In contrast, S3 has several parallel straight edge lines with diagonal orientation being placed in a parallel fashion with rather large in-between-distance, while S4 has the same number of them being placed in a parallel fashion with rather small in-between-distance. The experiments using S3 and S4 can show the behavior of the optimal scale selection with respect to influence of neighboring straight edges.

- The circular edge case

  We use three synthetic images representing three different types of a circular edge (see Fig. 2.2). C1 has a circular edge curve, whereas C2 and C3 contain several circular edge curves with two different in-between-distances. Analogously to the straight edge case, the experiments using C2 and C3 as compared with using C1 can expose

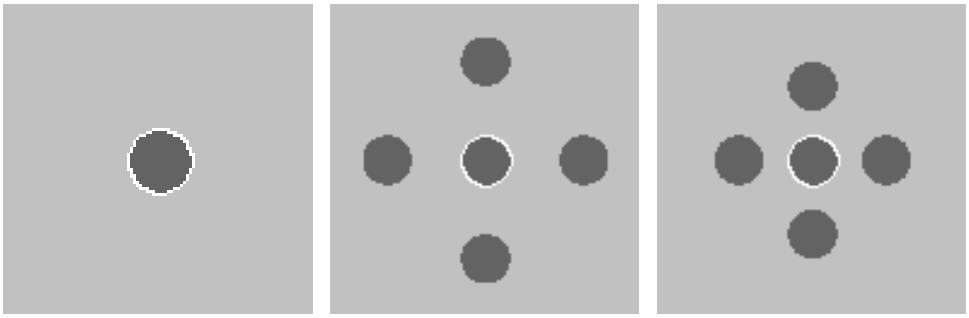

(a) C1 (b) C2 (c) C3

Figure 2.2: Synthetic images representing three different types of circular edge. The in-between-distance of neighboring circles in C2 corresponds to the diameter of the given circle, while the one of C3 corresponds to the radius of the given circle. The white curve marks the edge locus to be observed.

the behavior of the optimal scale selection with respect to influence of neighboring circular edge curves.

For a given edge width N, let us denote $\tau(N)$ a selected scale value resulting from the application of the developed framework for optimal scale selection. With respect to $\tau(N)$, we consider four indices, i.e. the *mean*, the *standard deviation*, the *maximum*, and the *minimum* of $\tau(N)$ along the edge line given as by

$$
\begin{aligned}
\overline{\tau}(N) &= \frac{1}{n_l}\sum_{l=1}^{l=n_l}\tau_l(N), \\
\tau_\sigma(N) &= \sqrt{\frac{1}{n_l}\sum_{l=1}^{l=n_l}(\tau_l(N)-\overline{\tau}(N))^2}, \\
\tau_{\max} &= \max_{1\le l\le n_l}\tau_l, \quad \text{and} \\
\tau_{\min} &= \min_{1\le l\le n_l}\tau_l,
\end{aligned}
\tag{2.1}
$$

where n_l corresponds to the total number of observed edge loci.

By comparing the experimental result of each type of edge, on one hand, we observe the behavior of the optimal scale selection with respect to orientation (in straight edge case

only), to the level of noise, and to the degree of in-between-distance of edge structure. On the other hand, through a comparison of the obtained experimental result with the theoretical result, we are able to assess how well the experimental results match the theoretical result. Note that the full range of experiments, e.g. by fine-sampling of the continuous parameter space, is beyond the scope of this thesis, and thus left to future work.

2.2 The Straight Edge Case

The theoretical result derived in [5, Sec. 5.2.1] is that an optimal scale value in straight edge extraction can be directly selected such that

$$S(t) = t^{\frac{1}{4}} \cdot M(t), \tag{2.2}$$

where t is the variance of the DSS kernel used for generating the scale-space representation and $M(t)$ corresponds to the magnitude of the gradient. A maximum of $S(t)$ along t is selected as an optimal scale. Note that, according to optimal scale selection based on 2.2, $\tau(N) = N$ must hold.

After describing the results of application of the developed optimal scale selection to each type of straight edge, we give an assessment on the experimental results compared with the theoretical result.

2.2.1 Experimental Results

The experimental results of the straight edge case are given Tab. 2.1-Tab. 2.4 as well as in Fig. 2.3-Fig. 2.6, where selected optimal scale values are given in terms of four indices given in Eq. 2.1.

For the case of S1, as marked in Fig. 2.1(a), 100 edge loci are observed. Tab. 2.1 shows selected optimal scale values. In case of S1 without noise (denoted as $\mathrm{S1}_{n0}$) given in Tab. 2.1(a),

$$\tau_{\mathrm{S1}_{n0}}(N) = N + 2 \quad \text{for any edge locus}$$

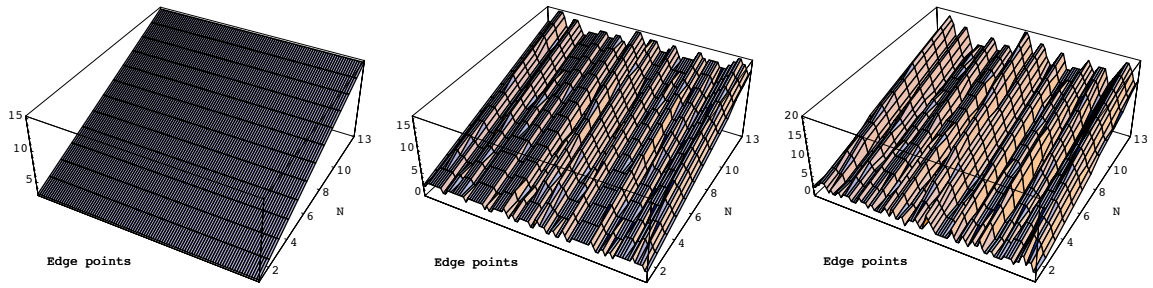

(a) $\tau_{\mathrm{S1}_{n0}}$ (b) $\tau_{\mathrm{S1}_{n5}}$ (c) $\tau_{\mathrm{S1}_{n10}}$

Figure 2.3: Selected scales through application of the optimal scale selection to S1.

holds for any N consistently (i.e. for a given edge width, the selected optimal scale values of edges along the edge line are identical). In other words, $\tau_{\mathrm{S1}_{n0}}(N)$ corresponds to $N+2$ consistently for any edge locus along the edge line, and thus $\tau_{\sigma,\mathrm{S1}_{n0}}(N) = 0$ for any N. In contrast, from the results of S1 with weak- and strong noise (denoted as $\mathrm{S1}_{n5}$ and $\mathrm{S1}_{n10}$, respectively) given in Tab. 2.1(b)-(c) it follows that optimal scale values are selected inconsistently (i.e. the standard deviation of optimal scale values selected along the edge line is not zero), though $\overline{\tau}_{\mathrm{S1}_{n5}}$ and $\overline{\tau}_{\mathrm{S1}_{n10}}$ are close to $\overline{\tau}_{\mathrm{S1}_{n0}}$. Note that $\tau_{\sigma,\mathrm{S1}_{n10}}$ is larger than $\tau_{\sigma,\mathrm{S1}_{n5}}$, which implies that optimal scales of edges along the edge line are selected more inconsistently as the level of noise becomes larger. This can be observed in Fig. 2.3.

As in the case of S1, 100 edge loci of S2 as marked in Fig. 2.1(b) are observed. In case of S2 without noise (denoted as $\mathrm{S2}_{n0}$) given in Tab. 2.2(a),

$$\tau_{\mathrm{S2}_{n0}}(N) = N + 1 \quad \text{for any edge locus}$$

holds. Similarly to the case of S1, from the results of S2 with weak- and strong noise (denoted as $\mathrm{S2}_{n5}$ and $\mathrm{S2}_{n10}$, respectively) given in Tab. 2.2(b)-(c) it follows that optimal scale values are selected inconsistently along the edge line, though $\overline{\tau}_{\mathrm{S2}_{n5}}$ and $\overline{\tau}_{\mathrm{S2}_{n10}}$ are close to $\overline{\tau}_{\mathrm{S2}_{n0}}$. Besides, one can see clearly in Fig. 2.4 that the larger the level of noise becomes the more inconsistently optimal scales of edges along the edge line are selected.

N	1	2	3	4	5	6	7	8	9	10	11	12	13
$\overline{\tau}(N)$	3.0	4.0	5.0	6.0	7.0	8.0	9.0	10.0	11.0	12.0	13.0	14.0	15.0
$\tau_\sigma(N)$	0.00	0.00	0.00	0.00	0.00	0.00	0.00	0.00	0.00	0.00	0.00	0.00	0.00
$\tau_{max}(N)$	3	4	5	6	7	8	9	10	11	12	13	14	15
$\tau_{min}(N)$	3	4	5	6	7	8	9	10	11	12	13	14	15

(a) $\mathrm{S1}_{n0}$

N	1	2	3	4	5	6	7	8	9	10	11	12	13
$\overline{\tau}(N)$	2.8	3.7	4.7	5.7	6.7	7.7	8.7	9.7	10.7	11.8	12.8	13.8	14.8
$\tau_\sigma(N)$	0.52	0.62	0.78	0.87	0.95	0.99	1.02	1.09	1.09	1.05	1.02	1.06	1.06
$\tau_{max}(N)$	4	5	7	8	9	10	11	12	13	14	15	16	17
$\tau_{min}(N)$	2	3	4	5	6	6	7	8	9	10	11	12	13

(b) $\mathrm{S1}_{n5}$

N	1	2	3	4	5	6	7	8	9	10	11	12	13
$\overline{\tau}(N)$	2.9	3.8	4.8	5.7	6.7	7.7	8.7	9.7	10.7	11.8	12.9	13.9	15.0
$\tau_\sigma(N)$	0.92	1.25	1.45	1.73	1.87	1.97	2.02	2.03	2.10	2.10	2.06	2.05	2.07
$\tau_{max}(N)$	6	7	8	10	11	12	13	14	15	16	17	19	20
$\tau_{min}(N)$	1	2	2	2	2	3	4	4	5	5	6	8	10

(c) $\mathrm{S1}_{n10}$

Table 2.1: Results obtained from applying the optimal scale selection to S1 in terms of $< \overline{\tau}, \tau_\sigma, \tau_{max}, \tau_{min} >$.

N	1	2	3	4	5	6	7	8	9	10	11	12	13
$\overline{\tau}(N)$	2.0	3.0	4.0	5.0	6.0	7.0	8.0	9.00	10.0	11.0	12.0	13.0	14.0
$\tau_\sigma(N)$	0.00	0.00	0.00	0.00	0.00	0.00	0.00	0.00	0.00	0.00	0.00	0.00	0.00
$\tau_{max}(N)$	2	3	4	5	6	7	8	9	10	11	12	13	14
$\tau_{min}(N)$	2	3	4	5	6	7	8	9	10	11	12	13	14

(a) $S2_{n0}$

N	1	2	3	4	5	6	7	8	9	10	11	12	13
$\overline{\tau}(N)$	2.0	2.9	3.9	4.9	5.9	6.9	7.9	8.8	9.9	10.8	11.8	12.8	13.8
$\tau_\sigma(N)$	0.17	0.36	0.51	0.63	0.78	0.87	1.01	1.04	1.09	1.26	1.28	1.34	1.46
$\tau_{max}(N)$	3	4	5	7	8	9	10	11	13	14	15	16	17
$\tau_{min}(N)$	1	2	3	4	4	5	5	6	7	7	8	9	9

(b) $S2_{n5}$

N	1	2	3	4	5	6	7	8	9	10	11	12	13
$\overline{\tau}(N)$	1.9	2.9	4.1	5.1	6.1	7.0	8.0	8.9	9.8	10.8	11.8	12.8	13.8
$\tau_\sigma(N)$	0.54	0.72	0.93	1.18	1.38	1.60	1.80	1.93	2.11	2.34	2.48	2.63	2.76
$\tau_{max}(N)$	4	5	7	8	10	11	13	14	15	17	18	19	20
$\tau_{min}(N)$	1	1	2	3	3	4	4	4	4	5	5	5	6

(c) $S2_{n10}$

Table 2.2: Results obtained from applying the optimal scale selection to S2 in terms of $< \overline{\tau}, \tau_\sigma, \tau_{max}, \tau_{min} >$.

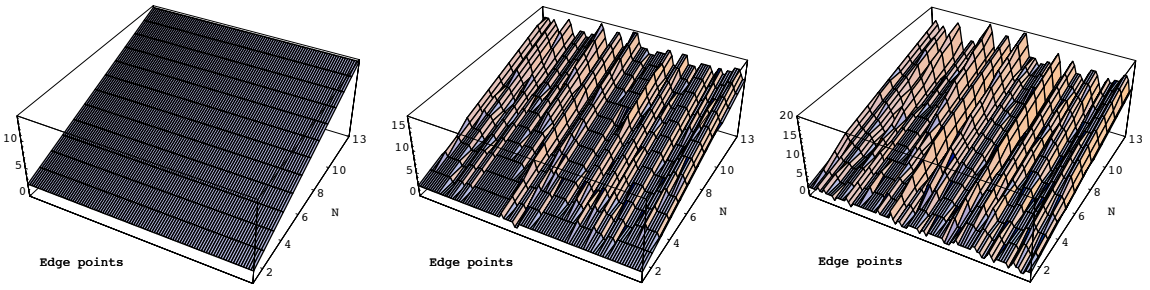

(a) $\tau_{\mathrm{S2}_{n0}}$ (b) $\tau_{\mathrm{S2}_{n5}}$ (c) $\tau_{\mathrm{S2}_{n10}}$

Figure 2.4: Selected scales through application of the optimal scale selection to S2.

Identically with the case of S2, 100 edge loci of S3 as marked in Fig. 2.1(c) are observed. Tab. 2.3(a) gives results for S3 without noise (denoted as $\mathrm{S3}_{n0}$)

$$\tau_{\mathrm{S3}_{n0}}(N) = N + 1 \quad \text{for any edge locus,}$$

which is equivalent to the result of $\mathrm{S2}_{n0}$. The results of S3 with weak- and strong noise (denoted as $\mathrm{S3}_{n5}$ and $\mathrm{S3}_{n10}$, respectively) are shown in Tab. 2.3(b)-(c), where optimal scale values are selected inconsistently along the edge line, though $\overline{\tau}_{\mathrm{S3}_{n5}}$ and $\overline{\tau}_{\mathrm{S3}_{n10}}$ are close to $\overline{\tau}_{\mathrm{S3}_{n0}}$. Moreover, consistency of selected optimal scales of edges along the edge line is getting worse as the level of noise becomes larger, which can be seen in Fig. 2.5.

Identically with the case of both S2 and S3, 100 edge loci of S4 as marked in Fig. 2.1(d) are observed. Tab. 2.4(a) gives results of S4 without noise (denoted as $\mathrm{S4}_{n0}$)

$$\tau_{\mathrm{S4}_{n0}}(N) = N + 1 \quad \text{for any edge locus,}$$

which is equivalent to the result of both $\mathrm{S2}_{n0}$ and $\mathrm{S3}_{n0}$. Tab. 2.4(b)-(c) give the results of S4 with weak- and strong noise (denoted as $\mathrm{S4}_{n5}$ and $\mathrm{S4}_{n10}$, respectively), which almost equal those of $\mathrm{S3}_{n5}$ and $\mathrm{S3}_{n10}$. Furthermore, similarly to the case of both S2 and S3, consistency of selected optimal scales of edges along the edge line is getting worse as the level of noise becomes larger, which is displayed in Fig. 2.6.

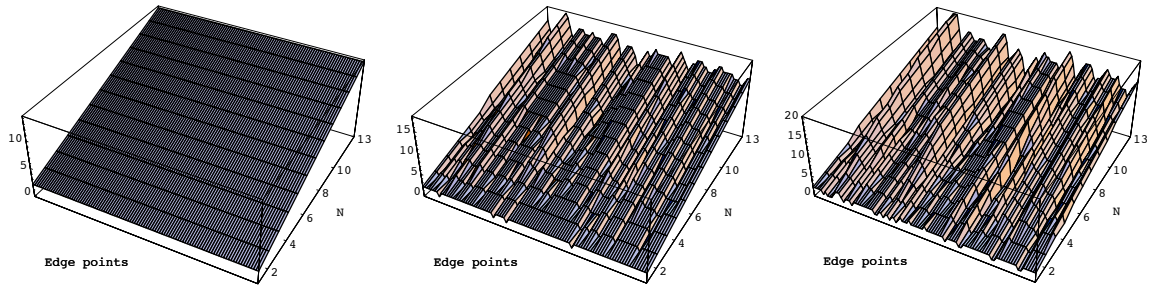

(a) $\tau_{\mathrm{S3}_{n0}}$ (b) $\tau_{\mathrm{S3}_{n5}}$ (c) $\tau_{\mathrm{S3}_{n10}}$

Figure 2.5: Selected scales through application of the optimal scale selection to S3.

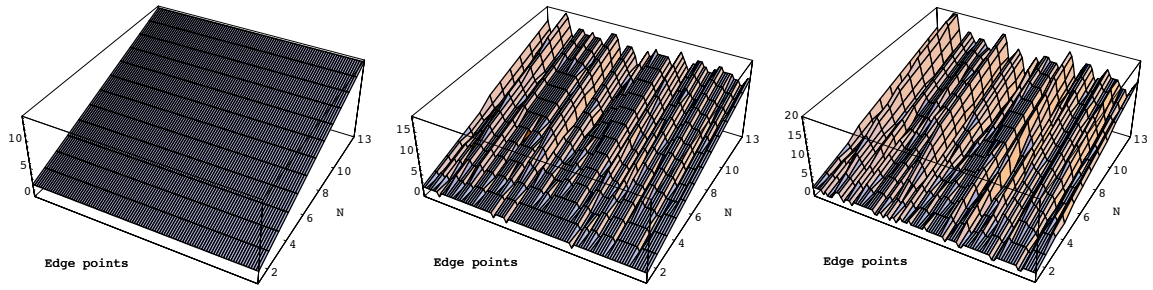

(a) $\tau_{\mathrm{S4}_{n0}}$ (b) $\tau_{\mathrm{S4}_{n5}}$ (c) $\tau_{\mathrm{S4}_{n10}}$

Figure 2.6: Selected scales through application of the optimal scale selection to S4.

N	1	2	3	4	5	6	7	8	9	10	11	12	13
$\overline{\tau}(N)$	2.0	3.0	4.0	5.0	6.0	7.0	8.0	9.00	10.0	11.0	12.0	13.0	14.0
$\tau_\sigma(N)$	0.00	0.00	0.00	0.00	0.00	0.00	0.00	0.00	0.00	0.00	0.00	0.00	0.00
$\tau_{max}(N)$	2	3	4	5	6	7	8	9	10	11	12	13	14
$\tau_{min}(N)$	2	3	4	5	6	7	8	9	10	11	12	13	14

(a) $S3_{n0}$

N	1	2	3	4	5	6	7	8	9	10	11	12	13
$\overline{\tau}(N)$	2.0	2.9	3.8	4.8	5.7	6.7	7.7	8.7	9.7	10.6	11.7	12.6	13.6
$\tau_\sigma(N)$	0.20	0.38	0.51	0.63	0.80	0.96	1.02	1.11	1.18	1.26	1.34	1.42	1.45
$\tau_{max}(N)$	2	4	5	6	8	9	11	12	13	14	16	17	18
$\tau_{min}(N)$	1	2	3	3	4	4	5	6	7	7	8	9	10

(b) $S3_{n5}$

N	1	2	3	4	5	6	7	8	9	10	11	12	13
$\overline{\tau}(N)$	1.9	2.7	3.7	4.7	5.6	6.6	7.6	8.6	9.6	10.5	11.5	12.4	13.4
$\tau_\sigma(N)$	0.47	0.71	0.99	1.25	1.60	1.73	1.94	2.11	2.30	2.50	2.61	2.73	2.87
$\tau_{max}(N)$	3	5	7	9	11	12	14	15	17	18	19	20	20
$\tau_{min}(N)$	1	1	2	2	2	3	3	3	3	3	4	4	4

(c) $S3_{n10}$

Table 2.3: Results obtained from applying the optimal scale selection to S3 in terms of $< \overline{\tau}, \tau_\sigma, \tau_{max}, \tau_{min} >$.

N	1	2	3	4	5	6	7	8	9	10	11	12	13
$\overline{\tau}(N)$	2.0	3.0	4.0	5.0	6.0	7.0	8.0	9.00	10.0	11.0	12.0	13.0	14.0
$\tau_\sigma(N)$	0.00	0.00	0.00	0.00	0.00	0.00	0.00	0.00	0.00	0.00	0.00	0.00	0.00
$\tau_{max}(N)$	2	3	4	5	6	7	8	9	10	11	12	13	14
$\tau_{min}(N)$	2	3	4	5	6	7	8	9	10	11	12	13	14

(a) $S4_{n0}$

N	1	2	3	4	5	6	7	8	9	10	11	12	13
$\overline{\tau}(N)$	2.0	2.9	3.8	4.8	5.7	6.7	7.7	8.7	9.7	10.6	11.7	12.6	13.6
$\tau_\sigma(N)$	0.20	0.38	0.51	0.63	0.80	0.96	1.02	1.11	1.18	1.26	1.34	1.42	1.45
$\tau_{max}(N)$	2	4	5	6	8	9	11	12	13	14	16	17	18
$\tau_{min}(N)$	1	2	3	3	4	4	5	6	7	7	8	9	10

(b) $S4_{n5}$

N	1	2	3	4	5	6	7	8	9	10	11	12	13
$\overline{\tau}(N)$	1.9	2.7	3.7	4.7	5.6	6.6	7.6	8.6	9.6	10.5	11.5	12.4	13.3
$\tau_\sigma(N)$	0.47	0.71	0.99	1.25	1.60	1.73	1.94	2.11	2.30	2.50	2.59	2.73	2.86
$\tau_{max}(N)$	3	5	7	9	11	12	14	15	17	18	19	20	20
$\tau_{min}(N)$	1	1	2	2	2	3	3	3	3	3	4	4	4

(c) $S4_{n10}$

Table 2.4: Results obtained from applying the optimal scale selection to S4 in terms of $< \overline{\tau}, \tau_\sigma, \tau_{max}, \tau_{min} >$.

2.2.2 Assessment

Fig. 2.7 gives a graphical illustration of the experimental results of both S1 and S2 in terms of $< \overline{\tau}, \tau_\sigma >$. In the noiseless case of Fig. 2.7,

$$\tau_{\mathrm{S1}_{n0}}(N) = N + 2 \quad \text{vs.} \quad \tau_{\mathrm{S2}_{n0}}(N) = N + 1$$

holds consistently for any N. Although it is difficult to account for the difference (i.e. one) between $\tau_{\mathrm{S1}_{n0}}$ and $\tau_{\mathrm{S2}_{n0}}$, it is obvious that there exists a slight difference in the results of optimal scale selection according to the different orientations of a straight edge. Besides, in the noisy case of Fig. 2.7, one can see that in general the larger the level of noise becomes the more inconsistent the result is, though $\overline{\tau}_{\mathrm{S1}_{\{n5,n10\}}}$ and $\overline{\tau}_{\mathrm{S2}_{\{n5,n10\}}}$ are close to $\overline{\tau}_{\mathrm{S1}_{n0}}$ and $\overline{\tau}_{\mathrm{S2}_{n0}}$, respectively. However, in particular the variation of $\tau_{\sigma,\mathrm{S2}_{\{n5,n10\}}}$ is relatively larger than $\tau_{\sigma,\mathrm{S1}_{\{n5,n10\}}}$ as the degree of edge width increases. This implies that, for a given large edge width, optimal scale selection for the vertical orientation of a noisy straight edge is relatively more consistent than for the diagonal orientation of a noisy straight edge.

One can find a graphical illustration of the experimental results of both S3 and S4 in terms of $< \overline{\tau}, \tau_\sigma >$ in Fig. 2.8, where

$$\tau_{\mathrm{S3}_{n0}}(N) = \tau_{\mathrm{S4}_{n0}}(N) = N + 1$$

holds consistently for any N, which is equivalent to the case of $\mathrm{S2}_{n0}$. In the noisy case of Fig. 2.8, the results of $\mathrm{S3}_{\{n5,n10\}}$ (see for detail Tab. 2.3) are highly similar to those of $\mathrm{S4}_{\{n5,n10\}}$ (see for detail Tab. 2.4), even though $\overline{\tau}_{\mathrm{S3}_{\{n5,n10\}}}$ and $\overline{\tau}_{\mathrm{S4}_{\{n5,n10\}}}$ are generally less close to $\overline{\tau}_{\mathrm{S2}_{n0}}$ than $\overline{\tau}_{\mathrm{S2}_{\{n5,n10\}}}$. This means that the neighboring noisy straight edges have a negative influence on the result of optimal scale selection. However, the degree of the in-between-distance has only a low effect on the result of optimal scale selection, where 'a low effect' is only valid in our experiment on condition that the in-between-distance of neighboring parallel straight edge lines should be larger than 20 pixels (see Fig. 2.1).

Tab. 2.5 summarizes the experimental results of each type of straight edge compared with the theoretical result illustrated in both Fig. 2.7 and Fig. 2.8. One can recognize from Tab. 2.5 that the obtained experimental results are close to the theoretical results

		S1	S2	S3	S4
Experimental result	noiseless	$\tau(N) = N+2$	$\tau(N) = N+1$	$\tau(N) = N+1$	$\tau(N) = N+1$
	weak noise	$\overline{\tau}(N) \approx N+2$	$\overline{\tau}(N) \approx N+1$	$\overline{\tau}(N) \approx N+1$	$\overline{\tau}(N) \approx N+1$
	strong noise	$\overline{\tau}(N) \sim N+2$	$\overline{\tau}(N) \sim N+1$	$\overline{\tau}(N) \sim N+1$	$\overline{\tau}(N) \sim N+1$
Theoretical result	$\tau(N) = N$				

Table 2.5: Comparison of the experimental results through application of the developed optimal scale selection to each type of straight edge with the theoretical result.

on the whole, though the experimental results slightly deviate from the theoretical ones. A close speculation about a definite reason of this slight deviation is beyond the scope of this thesis, however, we conjecture that it might be caused in part by an inevitable gap between a continuous theory and a discrete implementation. In particular, for each type of straight edge given here, a consistent result can be expected only in the case of noiseless images, whereas noisy images yield inconsistent result. This is due to the fact that the developed framework was derived on the basis of a the noiseless sigmoid edge model.

2.3 The Circular Edge Case

The theoretical result derived in [5, Sec. 5.2.2] is that an optimal scale value in circular edge extraction can be uniquely selected such that

$$S(t) = e^R \cdot M(t), \tag{2.3}$$

where R is the given radius of a circular edge, t is the variance of the DSS kernel used for generating the scale-space representation, and $M(t)$ corresponds to the magnitude of the gradient. Since the value of t satisfying $S(t) = I_1(R)$ ($I_1(\cdot)$ is the modified Bessel function of integer order 1) corresponds to $R - t_E$, the optimal scale (i.e. t_E) is selected by observing $S(t)$ along t. In other words, according to optimal scale selection based on Eq. 2.3, $\frac{\tau(N)}{3} = R - \frac{N}{3}$ viz. $\tau(N) = 3R - N$ must hold. Note that the developed framework is the first approach to optimal scale selection in circular edge extraction.

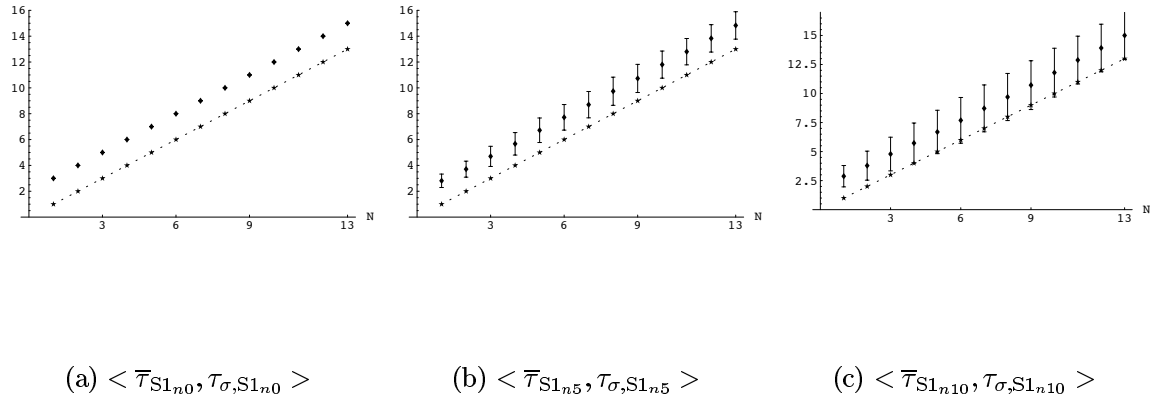

(a) $< \overline{\tau}_{\mathrm{S1}_{n0}}, \tau_{\sigma,\mathrm{S1}_{n0}} >$ (b) $< \overline{\tau}_{\mathrm{S1}_{n5}}, \tau_{\sigma,\mathrm{S1}_{n5}} >$ (c) $< \overline{\tau}_{\mathrm{S1}_{n10}}, \tau_{\sigma,\mathrm{S1}_{n10}} >$

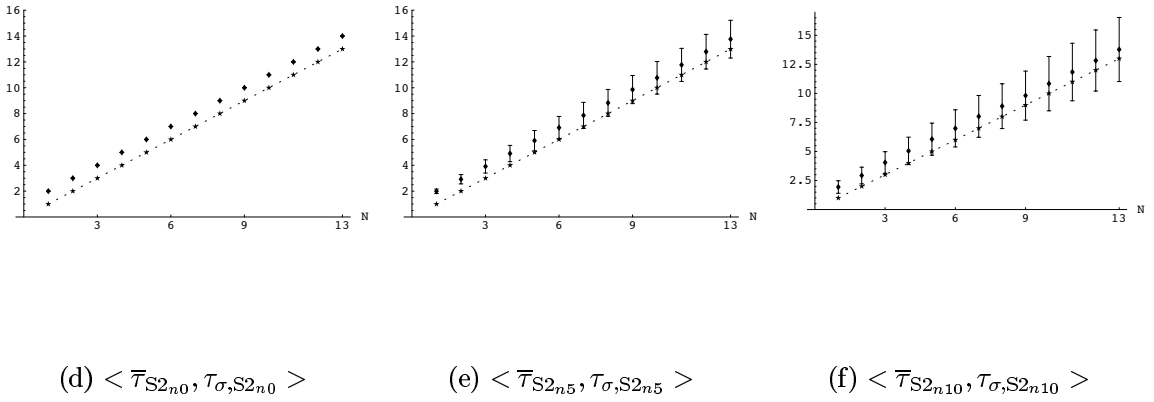

(d) $< \overline{\tau}_{\mathrm{S2}_{n0}}, \tau_{\sigma,\mathrm{S2}_{n0}} >$ (e) $< \overline{\tau}_{\mathrm{S2}_{n5}}, \tau_{\sigma,\mathrm{S2}_{n5}} >$ (f) $< \overline{\tau}_{\mathrm{S2}_{n10}}, \tau_{\sigma,\mathrm{S2}_{n10}} >$

Figure 2.7: Graphical illustration of experimental results of S1 and S2 compared with the theoretical result. Each row differs in the type of circular edge and each column differs in the level of noise. '$\cdots\bigstar\cdots$' corresponds to the theoretical result (i.e. $\tau(N) = N$), while '$\blacklozenge$' with error bar represents the experimental result.

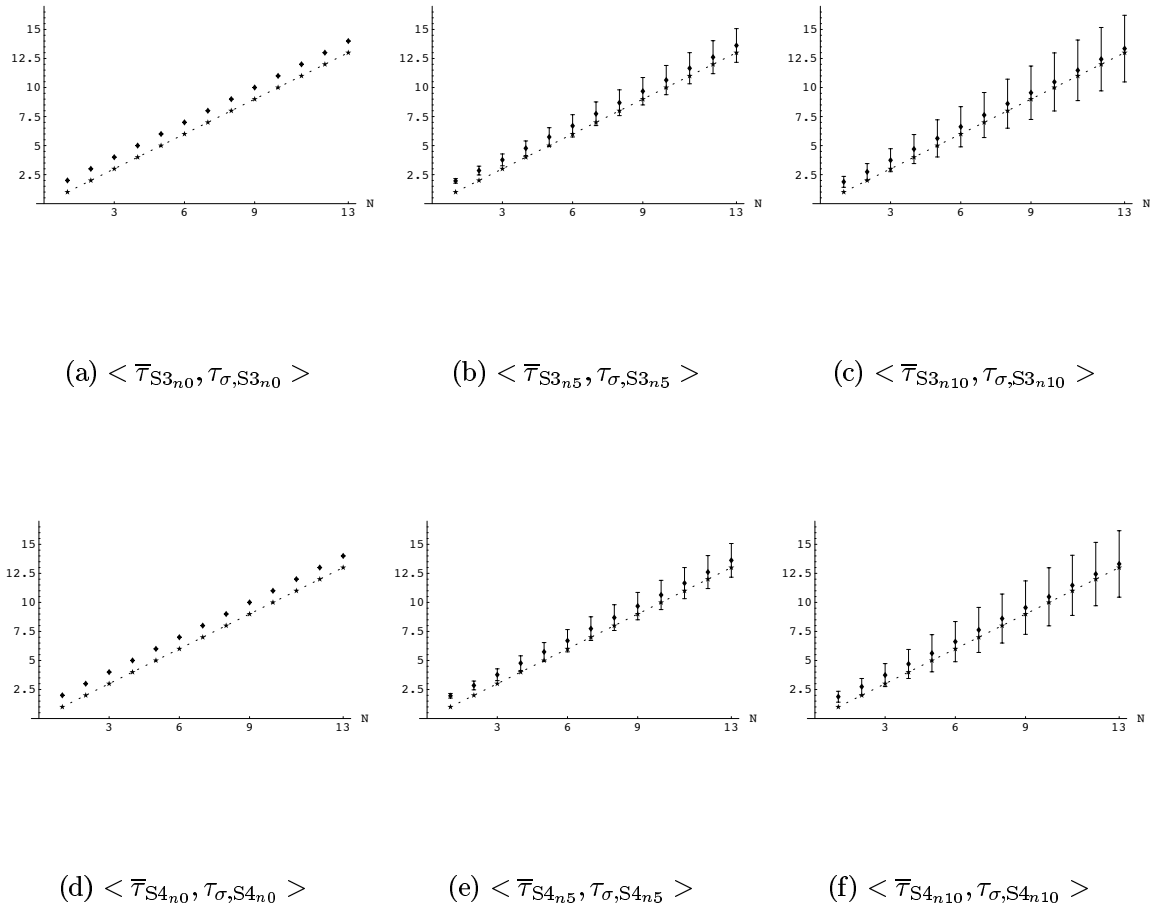

(a) $< \overline{\tau}_{\mathrm{S3}_{n0}}, \tau_{\sigma,\mathrm{S3}_{n0}} >$ (b) $< \overline{\tau}_{\mathrm{S3}_{n5}}, \tau_{\sigma,\mathrm{S3}_{n5}} >$ (c) $< \overline{\tau}_{\mathrm{S3}_{n10}}, \tau_{\sigma,\mathrm{S3}_{n10}} >$

(d) $< \overline{\tau}_{\mathrm{S4}_{n0}}, \tau_{\sigma,\mathrm{S4}_{n0}} >$ (e) $< \overline{\tau}_{\mathrm{S4}_{n5}}, \tau_{\sigma,\mathrm{S4}_{n5}} >$ (f) $< \overline{\tau}_{\mathrm{S4}_{n10}}, \tau_{\sigma,\mathrm{S4}_{n10}} >$

Figure 2.8: Graphical illustration of experimental results of S3 and S4 compared with the theoretical result. Each row differs in the type of straight edge and each column differs in the level of noise. '$\cdots\bigstar\cdots$' corresponds to the theoretical result (i.e. $\tau(N) = N$), while '$\blacklozenge$' with error bar represents the experimental result.

For the circular edge case, beside $< \overline{\tau}, \tau_\sigma, \tau_{\max}, \tau_{\min} >$ given in Eq. 2.1, we additionally examine the fit of $S(\tau(N))$ with $I_1(R)$ which we denote $\rho(N)$ defined as

$$\rho(N) = |I_1(R) - S(\tau(N))|, \tag{2.4}$$

where R is the given radius of a circular edge. $\rho(N)$ indicates how accurately $S(\tau(N))$ fits $I_1(R)$. According to the theoretical result of Eq. 2.3, $\rho(N) = 0$ must hold for any N. However, experimental results show that $\rho(N)$ hardly equals exactly zero. With respect to $\rho(N)$, we consider two indices i.e. the *mean* and the *standard deviation* of $\rho(N)$ along the edge curve given by

$$\begin{aligned} \overline{\rho}(N) &= \frac{1}{n_l} \sum_{l=1}^{l=n_l} \rho_l(N), \\ \rho_\sigma(N) &= \sqrt{\frac{1}{n_l} \sum_{l=1}^{l=n_l} (\rho_l(N) - \overline{\rho}(N))^2}, \end{aligned} \tag{2.5}$$

where n_l corresponds to the total number of observed edge loci along the circular edge curve.

After presentation of the results of applying the developed optimal scale selection to each type of circular edge, we give an assessment of the experimental results compared with the theoretical result.

2.3.1 Experimental Results

The experimental results of the circular edge case are given in Tab. 2.6-Tab. 2.8 as well as in Fig. 2.9-Fig. 2.11. The radius is given by $R = 10$ which corresponds to ten pixels. Selected scale values are given in terms of six indices shown in both Eq. 2.1 and Eq. 2.5.

For the case of C1, 70 edge loci as marked in Fig. 2.2(a) are observed clockwise. From both Tab. 2.6 and Fig. 2.9, one can see that the experimental results of C1 without noise (denoted as $\mathrm{C1}_{n0}$) as well as of C1 with weak- and strong noise (denoted as $\mathrm{C1}_{n5}$ and $\mathrm{C1}_{n10}$, respectively) are roughly close to the theoretical result (i.e. $\tau(N) = 3 \cdot 10 - N$), although the responses of $\tau(N)$ along the edge curves are not consistent. It is noticeable that $< \overline{\rho}, \rho_\sigma >$ of $\mathrm{C1}_{n0}$, $\mathrm{C1}_{n5}$, and $\mathrm{C1}_{n10}$ is in general quite small for any N.

N	1	2	3	4	5	6	7	8	9	10	11	12	13
$\overline{\tau}(N)$	27.68	26.68	25.68	24.68	23.68	22.68	21.68	20.68	19.68	18.68	17.68	16.68	15.68
$\tau_\sigma(N)$	1.53	1.53	1.53	1.53	1.53	1.53	1.53	1.53	1.53	1.53	1.53	1.53	1.53
$\tau_{max}(N)$	29	28	27	26	25	24	23	22	21	20	19	18	17
$\tau_{min}(N)$	24	23	22	21	20	19	18	17	16	15	14	13	12
$\overline{\rho}(N)$	0.46	0.46	0.46	0.46	0.46	0.46	0.46	0.46	0.46	0.46	0.46	0.46	0.46
$\rho_\sigma(N)$	0.22	0.22	0.22	0.22	0.22	0.22	0.22	0.22	0.22	0.22	0.22	0.22	0.22

(a) $\mathrm{C1}_{n0}$

N	1	2	3	4	5	6	7	8	9	10	11	12	13
$\overline{\tau}(N)$	28.10	27.11	26.11	25.08	24.10	23.08	22.10	21.13	20.11	19.10	18.10	17.14	16.17
$\tau_\sigma(N)$	1.40	1.42	1.42	1.43	1.44	1.44	1.46	1.49	1.50	1.51	1.53	1.59	1.61
$\tau_{max}(N)$	31	30	29	28	27	26	25	24	23	22	21	21	20
$\tau_{min}(N)$	24	23	22	21	20	19	18	17	16	15	14	13	12
$\overline{\rho}(N)$	0.49	0.49	0.49	0.49	0.49	0.49	0.48	0.47	0.46	0.46	0.46	0.47	0.48
$\rho_\sigma(N)$	0.24	0.23	0.23	0.24	0.24	0.24	0.25	0.26	0.26	0.26	0.27	0.25	0.24

(b) $\mathrm{C1}_{n5}$

N	1	2	3	4	5	6	7	8	9	10	11	12	13
$\overline{\tau}(N)$	28.32	27.31	26.35	25.35	24.35	23.37	22.41	21.44	20.44	19.42	18.44	17.46	16.35
$\tau_\sigma(N)$	1.64	1.65	1.68	1.71	1.80	1.83	1.88	1.96	2.02	2.06	2.17	2.20	2.34
$\tau_{max}(N)$	32	31	31	30	29	28	27	26	25	24	24	23	22
$\tau_{min}(N)$	25	24	23	22	21	20	19	18	17	16	15	14	12
$\overline{\rho}(N)$	0.43	0.43	0.43	0.42	0.43	0.44	0.44	0.44	0.45	0.46	0.45	0.49	0.53
$\rho_\sigma(N)$	0.24	0.25	0.26	0.26	0.24	0.24	0.26	0.26	0.25	0.26	0.27	0.24	0.23

(c) $\mathrm{C1}_{n10}$

Table 2.6: Results obtained from applying the optimal scale selection to C1 in terms of $< \overline{\tau}, \tau_\sigma, \tau_{max}, \tau_{min} >$ and $< \overline{\rho}, \rho_\sigma >$.

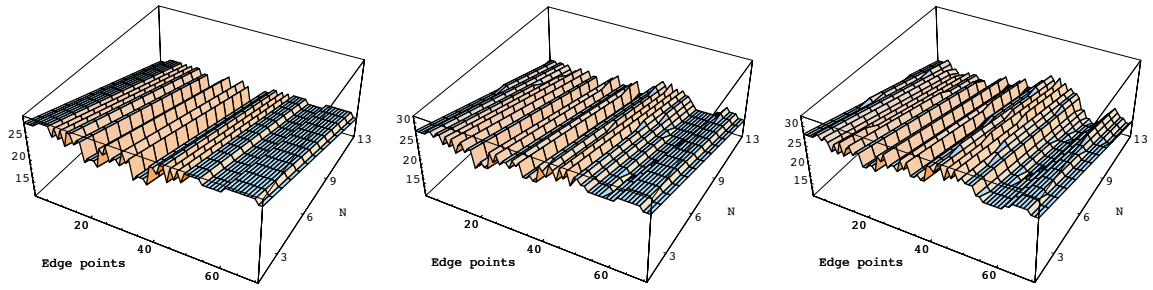

(a) $\tau_{\mathrm{C1}_{n0}}$ (b) $\tau_{\mathrm{C1}_{n5}}$ (c) $\tau_{\mathrm{C1}_{n10}}$

Figure 2.9: Selected scales through application of the optimal scale selection to C1.

As in the case of C1, 70 edge loci of C2 as marked in Fig. 2.2(b) are observed clockwise. The radius of the marked circle is equivalent to that of C1, and the in-between-distance of neighboring circles is the diameter ($D = 2R$) of the given circle (i.e $D = 20$ corresponding to 20 pixels). From both Tab. 2.7 and Fig. 2.10, one can see that the experimental results of $\mathrm{C2}_{n0}$, $\mathrm{C2}_{n5}$, and $\mathrm{C2}_{n10}$ are roughly close to the theoretical result, although the responses of $\tau(N)$ along the edge curves are not consistent for a given N. Also, the inconsistency of $\tau(N)$ seems to be getting larger as the level of noise becomes larger. However, $< \overline{\rho}, \rho_\sigma >$ of $\mathrm{C2}_{n0}$, $\mathrm{C2}_{n5}$, and $\mathrm{C2}_{n10}$ is in general quite small for any N.

As in the case of C2, 70 edge loci of C3 as marked in Fig. 2.2(c) are observed clockwise. The radius of the marked circle is equivalent to that of C2, and the in-between-distance of neighboring circles is the radius ($R = 10$) of the given circle (i.e $R = 10$ corresponding to 10 pixels). It is interesting to observe that the experimental results of the case of C3 shown in both Tab. 2.8 and Fig. 2.11 are very similar to those of the case of C2.

2.3.2 Assessment

Fig. 2.12 gives a graphical illustration of the experimental results of C1, C2, and C3 in terms of $< \overline{\tau}, \tau_\sigma >$ compared with the theoretical result.

One can notice several remarkable aspects from Fig. 2.12. First, the obtained experi-

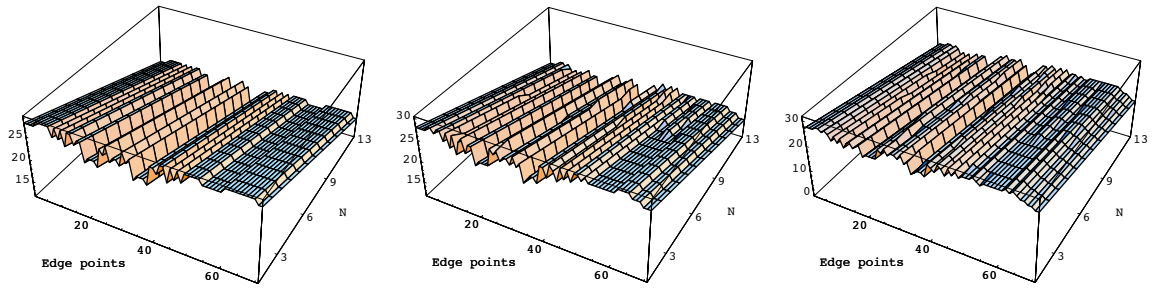

(a) $\tau_{\mathrm{C2}_{n0}}$ (b) $\tau_{\mathrm{C2}_{n5}}$ (c) $\tau_{\mathrm{C2}_{n10}}$

Figure 2.10: Selected scales through application of the optimal scale selection to C2.

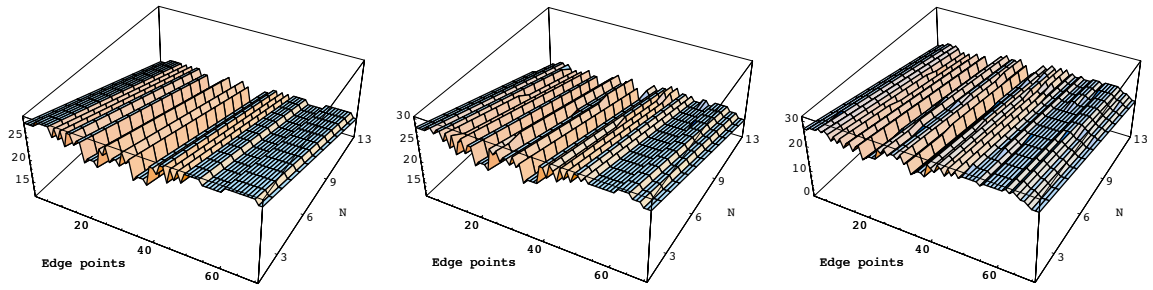

(a) $\tau_{\mathrm{C3}_{n0}}$ (b) $\tau_{\mathrm{C3}_{n5}}$ (c) $\tau_{\mathrm{C3}_{n10}}$

Figure 2.11: Selected scales through application of the optimal scale selection to C3.

N	1	2	3	4	5	6	7	8	9	10	11	12	13
$\overline{\tau}(N)$	27.68	26.68	25.68	24.68	23.68	22.68	21.68	20.68	19.68	18.68	17.68	16.68	15.68
$\tau_\sigma(N)$	1.53	1.53	1.53	1.53	1.53	1.53	1.53	1.53	1.53	1.53	1.53	1.53	1.53
$\tau_{max}(N)$	29	28	27	26	25	24	23	22	21	20	19	18	17
$\tau_{min}(N)$	24	23	22	21	20	19	18	17	16	15	14	13	12
$\overline{\rho}(N)$	0.46	0.46	0.46	0.46	0.46	0.46	0.46	0.46	0.46	0.46	0.46	0.46	0.46
$\rho_\sigma(N)$	0.22	0.22	0.22	0.22	0.22	0.22	0.22	0.22	0.22	0.22	0.22	0.22	0.22

(a) $C2_{n0}$

N	1	2	3	4	5	6	7	8	9	10	11	12	13
$\overline{\tau}(N)$	28.03	27.03	26.03	25.03	24.03	23.04	22.04	21.08	20.11	19.15	18.17	17.27	16.30
$\tau_\sigma(N)$	1.60	1.61	1.61	1.61	1.61	1.60	1.61	1.66	1.68	1.68	1.69	1.74	1.74
$\tau_{max}(N)$	30	29	28	27	26	25	24	23	22	21	20	20	19
$\tau_{min}(N)$	24	23	22	21	20	19	18	17	16	15	14	13	12
$\overline{\rho}(N)$	0.40	0.40	0.40	0.41	0.42	0.43	0.44	0.45	0.45	0.46	0.47	0.46	0.45
$\rho_\sigma(N)$	0.23	0.22	0.23	0.22	0.23	0.23	0.24	0.25	0.27	0.27	0.27	0.27	0.27

(b) $C2_{n5}$

N	1	2	3	4	5	6	7	8	9	10	11	12	13
$\overline{\tau}(N)$	28.24	27.31	26.31	25.32	24.34	23.38	22.41	21.48	20.49	19.35	18.62	17.66	16.68
$\tau_\sigma(N)$	1.86	1.87	1.92	1.95	1.96	1.97	2.01	2.03	2.06	2.95	2.20	2.21	2.29
$\tau_{max}(N)$	31	30	29	28	27	26	25	24	23	22	22	21	20
$\tau_{min}(N)$	24	23	22	21	20	19	18	17	16	2	13	12	10
$\overline{\rho}(N)$	0.50	0.50	0.50	0.50	0.49	0.49	0.49	0.50	0.51	0.50	0.47	0.43	0.43
$\rho_\sigma(N)$	0.26	0.26	0.25	0.24	0.24	0.25	0.25	0.25	0.25	0.27	0.27	0.26	0.27

(c) $C2_{n10}$

Table 2.7: Results obtained from applying the optimal scale selection to C2 in terms of $< \overline{\tau}, \tau_\sigma, \tau_{max}, \tau_{min} >$ and $< \overline{\rho}, \rho_\sigma >$.

N	1	2	3	4	5	6	7	8	9	10	11	12	13
$\overline{\tau}(N)$	27.68	26.68	25.68	24.68	23.68	22.68	21.68	20.68	19.68	18.68	17.68	16.68	15.68
$\tau_\sigma(N)$	1.53	1.53	1.53	1.53	1.53	1.53	1.53	1.53	1.53	1.53	1.53	1.53	1.53
$\tau_{max}(N)$	29	28	27	26	25	24	23	22	21	20	19	18	17
$\tau_{min}(N)$	24	23	22	21	20	19	18	17	16	15	14	13	12
$\overline{\rho}(N)$	0.39	0.39	0.39	0.39	0.39	0.39	0.39	0.39	0.39	0.39	0.39	0.39	0.39
$\rho_\sigma(N)$	0.20	0.20	0.20	0.20	0.20	0.20	0.20	0.20	0.20	0.20	0.20	0.20	0.20

(a) $\mathrm{C3}_{n0}$

N	1	2	3	4	5	6	7	8	9	10	11	12	13
$\overline{\tau}(N)$	27.99	26.97	25.99	25.01	24.01	23.03	22.01	21.04	20.04	19.07	18.08	17.14	16.17
$\tau_\sigma(N)$	1.67	1.67	1.68	1.63	1.63	1.61	1.62	1.62	1.62	1.65	1.65	1.71	1.73
$\tau_{max}(N)$	30	29	28	27	26	25	24	23	22	21	20	20	19
$\tau_{min}(N)$	24	23	22	21	20	19	18	17	16	15	14	13	12
$\overline{\rho}(N)$	0.41	0.41	0.41	0.42	0.43	0.43	0.44	0.45	0.45	0.46	0.47	0.48	0.48
$\rho_\sigma(N)$	0.29	0.29	0.28	0.27	0.26	0.25	0.25	0.24	0.25	0.26	0.27	0.27	0.27

(b) $\mathrm{C3}_{n5}$

N	1	2	3	4	5	6	7	8	9	10	11	12	13
$\overline{\tau}(N)$	28.14	27.15	26.15	25.21	24.23	23.25	22.31	21.37	20.37	19.23	18.52	17.58	16.55
$\tau_\sigma(N)$	1.94	1.95	1.98	2.01	2.02	2.02	2.02	2.04	2.04	2.93	2.23	2.26	2.30
$\tau_{max}(N)$	31	30	29	28	27	26	25	24	23	22	22	21	20
$\tau_{min}(N)$	23	22	21	20	19	18	18	17	16	2	13	12	10
$\overline{\rho}(N)$	0.47	0.46	0.45	0.44	0.44	0.44	0.45	0.48	0.52	0.52	0.52	0.49	0.47
$\rho_\sigma(N)$	0.25	0.26	0.28	0.29	0.29	0.30	0.28	0.26	0.26	0.27	0.25	0.24	0.26

(c) $\mathrm{C3}_{n10}$

Table 2.8: Results obtained from applying the optimal scale selection to C3 in terms of $< \overline{\tau}, \tau_\sigma, \tau_{max}, \tau_{min} >$ and $< \overline{\rho}, \rho_\sigma >$.

mental results are close to the theoretical results on the whole, though the experimental results do not coincide exactly with the theoretical one. The slightly inconsistent deviation of experimental results from the theoretical one may be rightfully assumed to be caused by an inevitable gap between a well-founded continuous theory and the implemented discrete case. In other words, even though the circular edge curves of the synthetic images used in our experiment were obtained from the mathematical equation of a circle, strictly speaking, they are not perfectly circular in a discretized image plane. Second, the experimental results are rarely affected by noise, compared with the straight edge case. This is because that the radius value of a circular edge plays a decisive role in optimal scale selection of developed framework (see Eq. 2.3) in which the selected optimal scale value mainly depends on the radius value, and thus the level of noise has on less influence on the circular edge case than on the straight edge case. Moreover, the degree of the in-between-distance has few effect on the result of optimal scale selection, which is only valid in our experiment on condition that the in-between-distance of neighboring circles should be larger than 10 pixels (see Fig. 2.2).

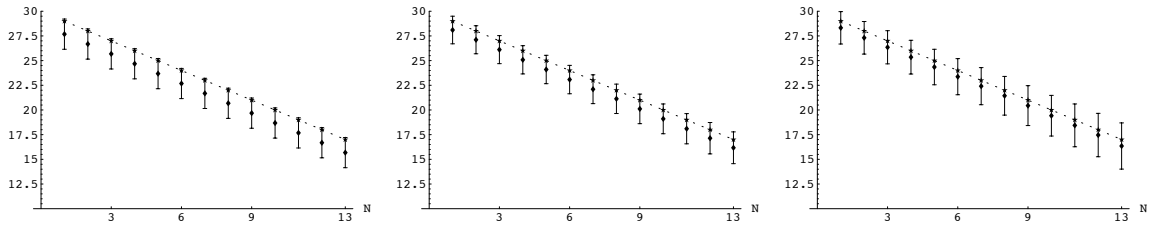

(a) $< \overline{\tau}_{\mathrm{C1}_{n0}}, \tau_{\sigma,\mathrm{C1}_{n0}} >$ (b) $< \overline{\tau}_{\mathrm{C1}_{n5}}, \tau_{\sigma,\mathrm{C1}_{n5}} >$ (c) $< \overline{\tau}_{\mathrm{C1}_{n10}}, \tau_{\sigma,\mathrm{C1}_{n10}} >$

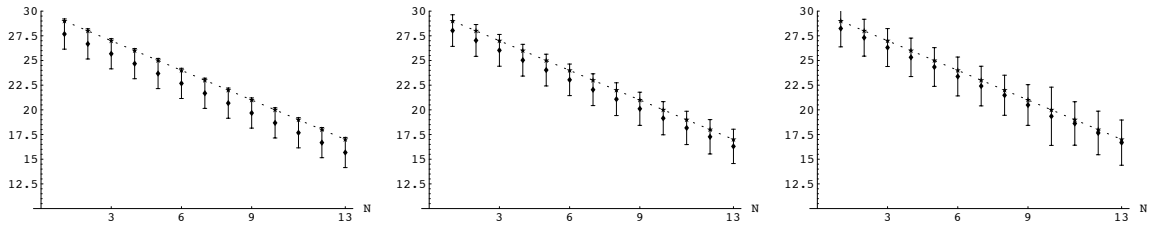

(d) $< \overline{\tau}_{\mathrm{C2}_{n0}}, \tau_{\sigma,\mathrm{C2}_{n0}} >$ (e) $< \overline{\tau}_{\mathrm{C2}_{n5}}, \tau_{\sigma,\mathrm{C2}_{n5}} >$ (f) $< \overline{\tau}_{\mathrm{C2}_{n10}}, \tau_{\sigma,\mathrm{C2}_{n10}} >$

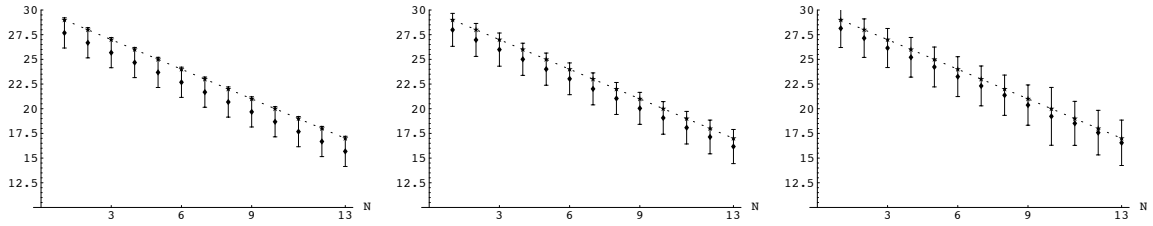

(g) $< \overline{\tau}_{\mathrm{C3}_{n0}}, \tau_{\sigma,\mathrm{C3}_{n0}} >$ (h) $< \overline{\tau}_{\mathrm{C3}_{n5}}, \tau_{\sigma,\mathrm{C3}_{n5}} >$ (i) $< \overline{\tau}_{\mathrm{C3}_{n10}}, \tau_{\sigma,\mathrm{C3}_{n10}} >$

Figure 2.12: Graphical illustration of experimental results of C1, C2, and C3 compared with the theoretical result. Each row differs in the type of circular edge and each column differs in the level of noise. '$\cdots\bigstar\cdots$' corresponds to the theoretical result (i.e. $\tau(N) = 30 - N$), while '$\blacklozenge$' with error bar represents the experimental result.

3 Summary

In this report, we presented the results of a validation study in which we investigated how well the experimental results obtained from application of the developed framework to an image match the theoretical result. It is worth noticing that this validation study is the first attempt for validating optimal scale selection approach in higher dimensional edge extraction, and thus its contribution should be understood as an exemplary stepping stone towards a fully fledged validation study.

In the straight edge case, the obtained experimental results are close to the theoretical results on the whole, though the experimental results slightly deviate from the theoretical ones. In particular, for each type of straight edge given here, a consistent result can be expected only with noiseless image, whereas noisy images yield inconsistent result. This is due to the fact that the developed framework was derived based on the noiseless sigmoid edge model. In the circular edge case, the obtained experimental results are again close to the theoretical results on the whole, though experimental results do not coincide exactly with the theoretical ones, which may be rightfully assumed to be caused by an inevitable gap between a well-founded continuous theory and the implemented discrete case. Furthermore, the experimental results are rarely affected by noise, as compared with the straight edge case. Both in the straight edge case and in the circular edge case, the degree of the in-between-distance of neighboring edge structures has only a low effect on the experimental result.

References

[1] J. F. Canny. A computational approach to edge detection. *IEEE Trans. on Pattern Analysis and Machine Intelligence*, 8(6):679–698, 1986.

[2] J. Y. Lim. On the Role of the Gaussian Kernel in Edge Detection and Scale-Space Methods. Technical Report FBI-HH-B-230/01, Fachbereich Informatik, Universität Hamburg, Germany, 2001.

[3] J. Y. Lim. On the Discrete Scale-Space Formulation. Technical Report FBI-HH-B-231/01, Fachbereich Informatik, Universität Hamburg, Germany, 2001.

[4] J. Y. Lim. The Supplemented Discrete Scale-Space Formulation. Technical Report FBI-HH-M-312/02, Fachbereich Informatik, Universität Hamburg, Germany, 2002.

[5] J. Y. Lim. On Higher Dimensional Multiscale Edge Extraction. Technical Report FBI-HH-B-238/02, Fachbereich Informatik, Universität Hamburg, Germany, 2002.

[6] J. Y. Lim. Validation of the DSS Kernel. Technical Report FBI-HH-B-241/02, Fachbereich Informatik, Universität Hamburg, Germany, 2002.

[7] T. Lindeberg. Scale-Space for Discrete Signals. *IEEE Trans. on Pattern Analysis and Machine Intelligence*, 12(3):234–264, 1990.